DR B R AMBEDKAR NATIONAL INSTITUTE OF TECHNOLOGY JALANDHAR-144011, INDIA
DEPARTMENT OF INDUSTRIAL AND PRODUCTION ENGINEERING
6th INTERNATIONAL CONFERENCE ON PRODUCTION AND INDUSTRIAL ENGINEERING
(CPIE-2019)

A NOVEL METHOD FOR SPINDLE RADIAL ERROR MEASUREMENT USING LASER POINTER AND DIGITAL CAMERA

Sanil Pande[1], Denis Ashok S[2]
[1-2] School of Mechanical Engineering
Vellore Institute of Technology, Vellore-632014, INDIA

ABSTRACT

This paper presents a machine vision system that utilizes a laser pointer mounted in the chuck and a camera that records the projected laser spot. An image processing methodology is developed to detect the laser spot while operating a lathe at different speeds. The centroid of the spot is calculated using image moments to obtain its coordinates, and shape matching using Hu moments is performed to validate the detection. A mathematical analysis of the coordinates using curve fitting to a Fourier Series is implemented in order to obtain the synchronous and asynchronous spindle radial errors. The synchronous error is found to follow a periodic pattern and the errors are found to increase with respect to operating speed. The harmonic components of spindle radial error are thus measured and presented.

1. INTRODUCTION

A spindle refers to the rotating part installed in the headstock of a lathe. Spindle error can be attributed to internal causes in the machine such as misaligned bearings, out-of-round bearings, structural vibrations and general wear and tear over time. ANSI/ASME Axes of Rotation: Methods for Specifying and Testing provides the standards for measurement, specifications and testing of the synchronous and asynchronous errors in rotating machine tools [1]. A mathematical model approach to separate the centering error and synchronous components of spindle radial errors is presented in [2]. In [3], a machine vision system using circular Hough transform to detect the center of a cylindrical workpiece is implemented to measure the form error of the master cylinder and the components of spindle radial error. The detection of a laser spot based on the hue and value corresponding to the brightest spot in an image has been implemented in [4]. Methods to detect the laser spot include thresholding and background subtraction, and subsequent coordinate mapping of the obtained coordinates [5]. In [6], the use of modified circular Hough transforms in which gradients are not assumed to converge at a single point for detecting laser spots in images is proposed. In [7] , laser spots were detected using background subtraction and noise removal, and laser spot tracking was performed by implementing an improved Kalman filtering algorithm. In this work, image processing using masking, closing and noise removal is implemented and Fourier series curve-fitting is used to segregate synchronous and asynchronous spindle errors.

2. METHODOLOGY

2.1 Experimental Setup

The proposed machine vision system consists of a camera, a laser pointer and a surface on which the laser spot is projected, as shown in figure 1. The camera utilized is inbuilt in the OnePlus 5T smartphone and it captures video at a resolution of 1920x1080 pixels at a rate of 30.04 frames per second. The laser pointer uses a laser diode to emit light of wavelength 630-680 nm. It is a class IIA laser with a power output less than 1 mW. The projected spot follows a Gaussian profile. A matte black surface is chosen to project the laser spot on since

it limits the reflectivity of the laser beam resulting in a coherent laser spot for image processing. The distance between the laser emitter and the perpendicular surface is measured to be 16.7 cm using a regular scale. The distance between the camera and the surface is 16.6 cm. The resultant angle between the focal axis of the camera and the spindle axis is 6.3°.

Figure 1(a). Laser Pointer and Projected Spot

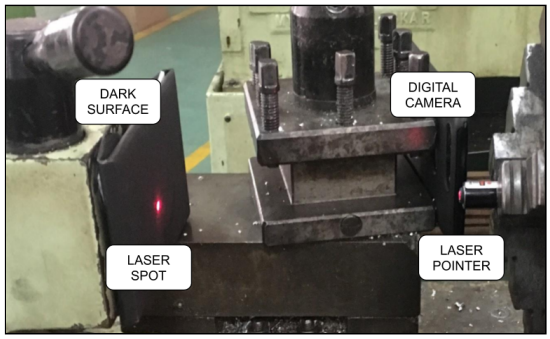

Figure 1(b). Camera Setup Schematic

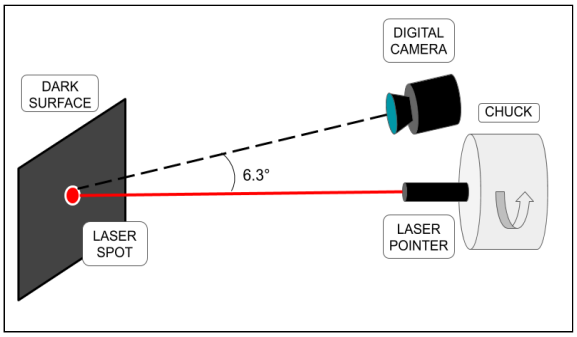

2.2 Conversion of pixels to real world measurements

Images of slip gauges were captured at a distance equal to 16.5 cm, equivalent to the original setup. An image of a slip-gauge of length 100 mm and breadth 35 mm was taken, and the pixel coordinates of the corners were obtained. The perimeter of the rectangle thus formed was found to be equal to 3271.22 pixels, corresponding to a perimeter of 270mm of the slip gauge.The conversion factor was thus found to be 0.08254 mm/pixel or 82.54 µm/pixel.

2.3 Colour Thresholding and Binarization

The image processing is performed using the Python programming language with its open source computer vision library, OpenCV. The frames in the video are cropped to a region of interest of 960x540 pixels which encompasses the range of motion of the laser spot. A masking operation is performed on each frame on the to extract red pixels. The masking values are between [0,0,250] and [160,255,255] in the hue-saturation-value colour space. Upon thresholding, a binarized image is obtained which has a pixel value of 1 corresponding to the red pixels in the original image, resulting in a clear demarcation of the laser spot from its background as shown in figure 2.

Figure 2(a). Cropped Region of Interest

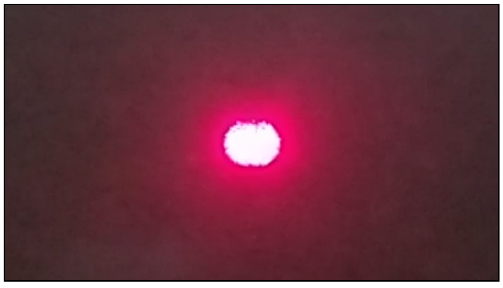

Figure 2(b). Masked Image

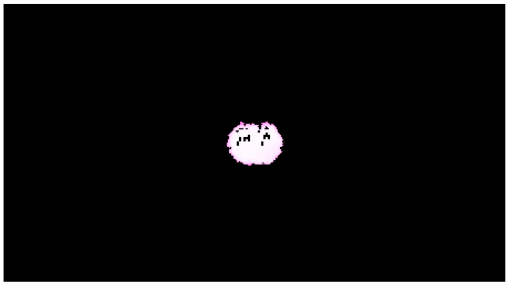

2.4 Closing Morphological Operation

The laser spot has some concavity due do a defect in the emitting diode as shown in figure 3(a). To compensate for this, a closing morphological operation with a kernel size of 25x25 pixels is applied. The closing operation is performed by dilation and then erosion of an image, as described in (1) and (2), where x’ and y’ are half of the kernel size i.e. 12 pixels.

$$f_{dilation}(x,y) = max_{(x',y')\neq 0}\ img(x+x', y+y') \quad (1)$$

$$f_{erosion}(x,y) = min_{(x',y')\neq 0}\ img(x+x', y+y') \quad (2)$$

The result is a convex laser spot with a consistent shape as shown in figure 3(b).

Figure 3(a). Binarized Image

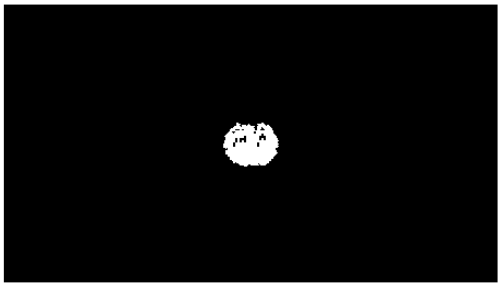

Figure 3(b). Closing Operation

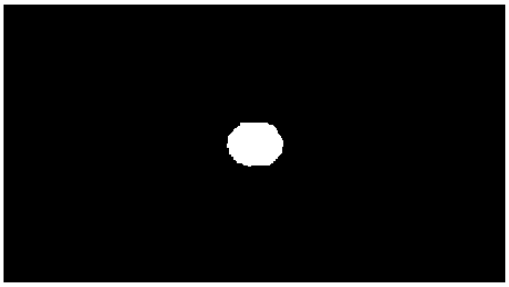

2.5 Noise Removal with Gaussian Blur

In order to remove noise and smoothen the edges of the laser spot, the image is correlated with a kernel of size 7x7 pixels, the elements of which are an approximation of a Gaussian function in two dimensions given by (3). The denoised image with smoothed edges is shown in figure 4.

$$G(x,y) = \frac{1}{2\pi\sigma^2}\, e^{\frac{(x^2+y^2)}{2\sigma^2}} \quad (3)$$

2.6 Laser Spot Detection

In order to measure the pixel coordinates of the laser spot, we calculate the centroid of the image which is equivalent to the centroid of the laser spot. The X and Y coordinates of the centroid of an image are calculated using the image moments, as given in (4).

$$\{\bar{x}, \bar{y}\} = \left\{\frac{M_{10}}{M_{00}}, \frac{M_{01}}{M_{00}}\right\} \quad (4)$$

Where M_{00} denotes the area of the laser spot and M_{10} and M_{01} denote the raw moment of the image in the x and y directions, respectively. The detected centroid is denoted by the green dot as shown in figure 4.

Figure 4. The centroid marked by a green dot.

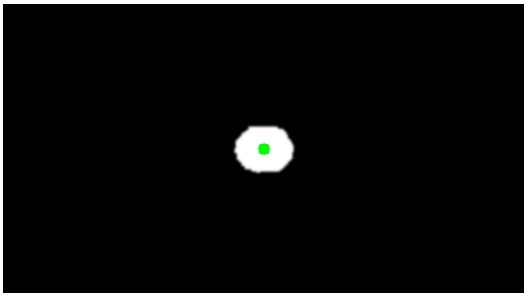

2.7 Fourier Analysis of Coordinates

A Fourier Series curve fitting is performed on the collected X and Y coordinates using the sum of least squares method. The general Fourier Series equation is used, up to the fifth harmonic. The general form of a Fourier Series equation is given by (5).

$$f(t_i) = a_0 + \sum_{h=1}^{H} (a_h cos(w * h * t_i) + b_h sin(w * h * t_i)) \quad (5)$$

The curve fitting of the X and Y coordinates of the laser spot with respect to time provides us with the following parametric coefficients in table 1.

Table 1. Fourier series coefficients obtained by least square curve fitting.

Parametric Coefficients	a0	a1	b1	a2	b2	a3	b3	a4	b4	a5	b5	w
X (45 RPM)	0.0498	-2.503	-0.9678	0.0155	0.0146	-0.0149	0.0170	-0.0003	-0.0038	-0.0020	-0.0130	5.016
Y (45 RPM)	-0.0033	-0.9437	2.567	0.0169	-0.0075	-0.0160	-0.0057	-0.0001	0.0023	-0.0102	0.0018	5.016
X (71 RPM)	-0.0594	-2.461	2.091	0.0080	-0.0252	0.0049	-0.0148	0.0027	-0.0048	0.0036	-0.0035	7.952
Y (71 RPM)	-0.0642	2.188	2.468	-0.0281	-0.0148	0.0194	0.0119	-0.0040	0.0008	0.0040	-0.0046	7.953

The dominant frequencies are a_0, a_1 and b_1 which the centering error can be attributed to. The remaining frequencies from the second harmonic onwards contribute to the synchronous error. The residual error is used to determine the asynchronous errors in the lathe.

3. RESULTS AND DISCUSSIONS

3.1 Laser Spot Detection

The consistency of the shape of the laser spot can be verified by calculating the Hu moments of the image. This gives us 7 moments of increasing order for the detected spot in each frame, which depend on the shape of the image and are translation, scale and rotation invariant [8]. The $\log_{10}$ of the calculated moments for 5 consecutive frames are given in table 2. The change of sign across the seventh moment denotes that the shape is a mirror image of the preceding frame, which is consistent with the fact that the laser spot is symmetric and thus the same as its mirror image. The similarity of the moments across frames is indicative of the robustness of the laser spot detection method used, as shown in [9].

Table 2. Hu Moments calculated for successive frames

Hu Moments	Frame 1	Frame 2	Frame 3	Frame 4	Frame 5	Deviation (magnitude)
Moment #1	3.177565	3.177388	3.176317	3.172763	3.176592	0.15%
Moment #2	7.469690	7.519065	7.543288	7.466522	7.481772	1.02%
Moment #3	11.868214	12.321896	12.204218	12.461534	12.227923	4.86%
Moment #4	13.114282	13.231826	12.900100	13.034997	13.139142	2.54%
Moment #5	-25.637807	-26.121476	-25.454779	-25.792012	-25.849473	2.59%
Moment #6	-16.856538	-16.992348	-16.708980	-16.816648	-16.984048	1.68%
Moment #7	26.035402	26.204890	-26.421183	-26.485036	-26.290253	1.71%

3.2 Synchronous Error

The synchronous errors are obtained from the second to fifth harmonics of the curve fitted Fourier Series in table 1. The polar plots are observed to follow a similar shape at different speeds, suggesting that the synchronous error is a periodic function of the angular displacement. The offset in the plots is due to the change in the starting position during the experiment, since the relative angular displacement is considered. The amplitude of the synchronous error is found to be 79.5 microns at 45 RPM and 92.7 microns at 71 RPM.

Figure 4(a). Error (in mm) at 45 RPM

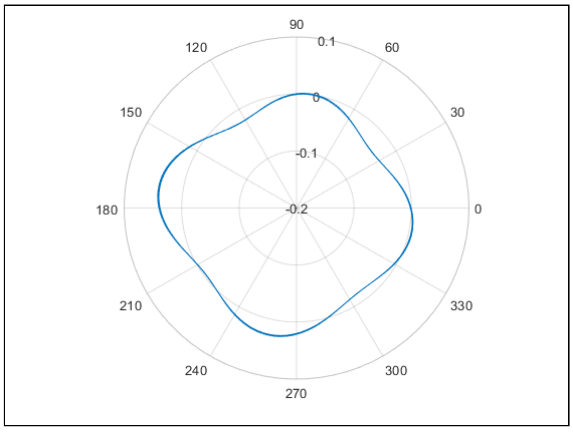

Figure 4(b). Error (in mm) at 71 RPM

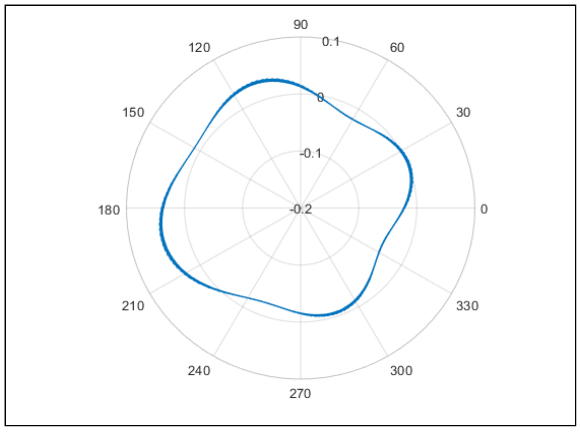

3.4 Asynchronous Error

The asynchronous error which is caused by random errors in the lathe is obtained through the curve fitting residuals. It is found to vary randomly, as shown in the polar plot in figure 5. The amplitude of error is 233.2 microns at 45 RPM and 319.4 microns at 71 RPM.

Figure 5(a). Error (in mm) at 45 RPM

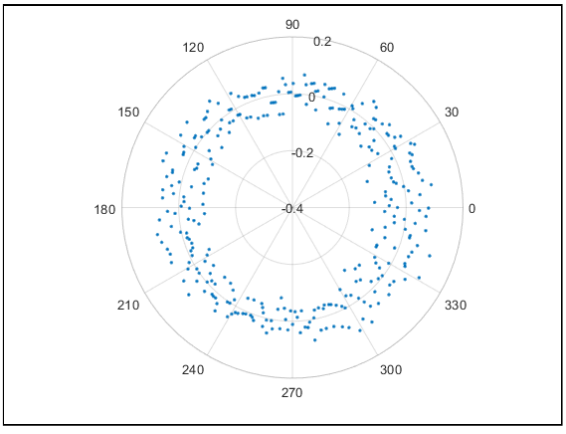

Figure 5(b). Error (in mm) at 71 RPM

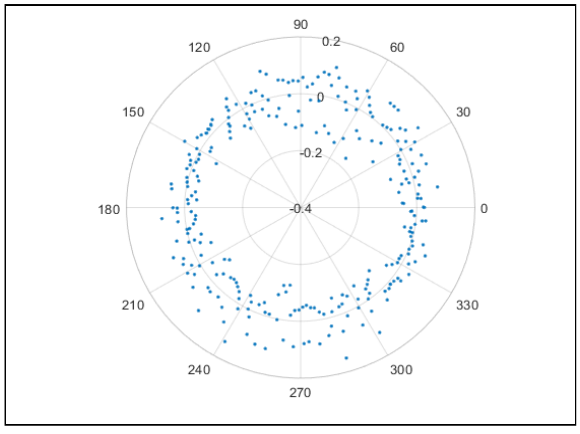

3.5 Combined Spindle Radial Error

The amplitude of both synchronous and asynchronous errors is found to increase with an increase in the operating speed of the lathe. The contribution of the synchronous error is found to be lesser compared to that of the asynchronous error towards the combined error. The error measurements are given in table 3.

Table 3. Measurements of Synchronous and Asynchronous Spindle Error

Type of Error	Synchronous Error		Asynchronous Error		Combined Error	
	45 RPM	71 RPM	45 RPM	71 RPM	45 RPM	71 RPM
Minimum Value (μm)	-36.4	-46.3	-121.6	-167.5	-145.2	-182
Maximum Value (μm)	43.1	46.4	111.6	151.9	117.6	147.5
Amplitude (μm)	79.5	92.7	233.2	319.4	262.8	329.5

4. CONCLUSIONS

A general method of detecting laser spots through the use of computer vision is developed. These operations which involve masking, binarization, closing and blurring are observed to be robust in the detection and tracking of the laser spot, as shown by the consistency in the Hu moments through successive frames. The synchronous error is found to vary between 50μm and 100μm, while the asynchronous and combined errors vary between 200μm and 350μm. The synchronous, asynchronous and combined errors are found to increase at higher operating speeds. It is observed that the synchronous error is a periodic function due to the inherent errors in the spindle. The proposed method can be used as a low-cost implementation for the testing of machine tool spindles.

REFERENCES

1. Axes of rotation: methods for specifying and testing. American Society of Mechanical Engineers, New York, NY (2010).
2. Ashok, S., Samuel, G.: Modeling, measurement, and evaluation of spindle radial errors in a miniaturized machine tool. The International Journal of Advanced Manufacturing Technology. 59, 445-461 (2011).
3. Kavitha, C., Ashok, S.: A New Approach to Spindle Radial Error Evaluation Using a Machine Vision System. Metrology and Measurement Systems. 24, 201-219 (2017).
4. Mesko, M., Toth, S.:Laser Spot Detection. Journal of Information, Control and Management Systems. 11(1), 35-42 (2013).
5. Zakaria, N. F., Zulkifley, M.A., Mustafa, M.M. and Abdul Karim R.: A review on Laser Spot Detection System Based on Image Processing Techniques. Journal of Theoretical and Applied Information Technology. 70(2), 333-344 (2014).
6. Krstinić, D., Skelin, A., Milatić, I.: Laser Spot Tracking Based on Modified Circular Hough Transform and Motion Pattern Analysis. Sensors. 14, 20112-20133 (2014).
7. Ahmed, F., Maryam, M.: Laser Spot Detection and Tracking. Zanco Journal of Pure and Applied Sciences. 28(2), 615-623 (2016).
8. Hu, M.: Visual pattern recognition by moment invariants. IEEE Transactions on Information Theory. 8, 179-187 (1962).
9. Huang, Z., Leng, J.: Analysis of Hu's moment invariants on image scaling and rotation. 2nd International Conference on Computer Engineering and Technology. 7, 476-480 (2010).